PHILOSOPHICAL MAGAZINE
https://doi.org/10.1080/14786435.2020.1771454

Taylor & Francis
Taylor & Francis Group

Mechanistic model for the dielectric spectrum of a simple dielectric material

Solvej Knudsen, Jeppe C. Dyre and J. S. Hansen

'Glass and Time', IMFUFA, Department of Science and Environment, Roskilde University, Roskilde, Denmark

ABSTRACT

In this paper, we perform molecular dynamics simulations of a dielectric fluidic material composed of permanent molecular dipoles. The dielectric spectrum features two peaks at lower frequencies than the system phonon frequency. The primary peak is observed at all temperatures studied and shifts toward lower frequencies as the temperature decreases. During this shift, the secondary peak emerges with a higher peak frequency than the primary peak. The secondary peak amplitude increases as the temperature decreases. Both peaks are dependent on the wavevector; in the small wavevector regime, the primary peak is shifted to higher frequencies as the wavevector squared and the secondary peak amplitude increases as the wavevector increases, but shows no shift in frequency. From the polarisation balance equation, we propose a model for the dielectric spectrum. This captures the spectrum features, and we conjecture that the primary peak is due to dipole moment correlations (Debye-type) and the secondary peak is due to the correlation between the dipole moment and a microscopic local field.

ARTICLE HISTORY
Received 15 October 2019
Accepted 13 May 2020

KEYWORDS
Dielectric materials; molecular dynamic simulations; polarisation; amorphous materials

1. Introduction

Application of an external electric field to a dielectric material gives rise to a polarisation density, $\mathbf{P}$, of the material. For sufficiently small fields, the polarisation is linear with respect to the field [1], and in the zero frequency and wavevector limit, homogeneous and isotropic case we have the simple constitutive relation

$$\mathbf{P} = \varepsilon_0 \chi_e \mathbf{E}, \tag{1}$$

where ε_0 is the dielectric permittivity of vacuum, χ_e is the dielectric susceptibility, and $\mathbf{E}$ is the local electric field. The dielectric susceptibility is often expressed in terms of the relative permittivity, $\varepsilon_{r,0}$, as $\chi_e = \varepsilon_{r,0} - 1$, where the

CONTACT J. S. Hansen jschmidt@ruc.dk 'Glass and Time', IMFUFA, Department of Science and Environment, Roskilde University, Postbox 260, Roskilde DK-4000, Denmark

subscript indicates that this expression is true in the zero frequency and zero wavevector limit. In general, the dielectric response depends on both the applied field history and local spatial correlations [2, 3]. The linear constitutive relation, Equation (1), can then be generalised by introducing a wavevector and frequency dependent susceptibility or, equivalently, a wavevector and frequency dependent relative permittivity, $\varepsilon_r = \varepsilon_r(\mathbf{k}, \omega)$.

At zero wavevector the dielectric spectrum, i.e. the function $\varepsilon_r(\omega) = \varepsilon_r(\mathbf{0}, \omega)$, has been intensively studied for decades [4–7]. The imaginary part of the spectrum (the dielectric loss) is observed to have many interesting features, especially, upon system cooling, see for example Refs. [8–10]. The underlying physical processes responsible for the rich dynamics are still not clear [10–12], and are likely to depend on the specific molecular system under investigation [13].

The material dielectric properties can also be studied in equilibrium [14]. Here the local polarisation density will fluctuate due to the system thermal energy and the dynamics of the fluctuations can be studied through their correlations. The fluctuation–dissipation theorem shows that the permittivity is in general given through the bound charge density correlations [15], but in the small frequency and wavevector regime this coincide with the polarisation correlations [14, 15], hence, the polarisation is a fundamental quantity to study in order to understand the underlying physical mechanisms.

By means of the polarisation fluctuations, we here investigate the wavevector and frequency dependent dielectric properties for a simple fluidic material. By the term *simple material* we imply a material that is made of permanent molecular (or microscopic) rigid dipoles with only translational and rotational degrees of freedom. In this way we can ignore any effects from induced dipole moments and intra-molecular re-arrangements, which allows us to propose a model for the polarisation density from which one can derive the dielectric properties in the limit of small frequency and wavevector. The model for the spectrum is compared to results from molecular dynamics simulations of the material.

2. Model of the dielectric spectrum

The dynamical equations for the relevant correlation functions have been derived by Hansen [16]. For completeness and ease of reading we will here present the derivation. First, we write the polarisation density in terms of the mass density, ρ, and the dipole moment per unit mass $\mathbf{p}$ as $\mathbf{P}(\mathbf{r}, t) = \rho(\mathbf{r}, t)\mathbf{p}(\mathbf{r}, t)$. The balance equation for the polarisation at low wavevector is then given by [16]

$$\frac{\partial(\rho\mathbf{p})}{\partial t} + \nabla \cdot \big(\rho\mathbf{u}\mathbf{p}\big) = \frac{1}{\tau_P}\big(\kappa\mathbf{E} - \rho\mathbf{p}\big) + \rho(\boldsymbol{\Omega} \times \mathbf{p}) - \nabla \cdot \mathbf{R}, \tag{2}$$

where $\mathbf{u}$ is the streaming velocity, τ_P is the characteristic polarisation relaxation time, κ is the polarisability, $\mathbf{E}$ is an electric field we define below, $\boldsymbol{\Omega}$ is the angular velocity, and $\mathbf{R}$ is the dipole flux tensor. Notice that in Ref. [16] κ is the polarisability per unit mass and is related to the current definition by a factor of density. Hansen [16] proposed the following constitutive relation for $\mathbf{R}$

$$\mathbf{R} = -\chi_v(\nabla \cdot \mathbf{p})\mathbf{I} - 2\chi_0(\overset{os}{\nabla}\mathbf{p}) - 2\chi_r(\overset{a}{\nabla}\mathbf{p}) + \delta\mathbf{R}. \tag{3}$$

Here χ_v, χ_0, and χ_r are phenomenological transport coefficients, and $\mathbf{I}$ is the 3×3 identity tensor. Superscripts *os* and *a* indicate the traceless symmetric and anti-symmetric parts of the tensor $\nabla\mathbf{p}$, respectively. $\delta\mathbf{R}$ denotes the fluctuating part of the dipole flux and has the property that each tensor component, δR_{nm}, has zero mean and is uncorrelated with any component in the dipole moment, that is,

$$\langle \delta R_{nm} \rangle = 0 \quad \text{and} \quad \langle \delta R_{nm}(\mathbf{r}, t)\, p_l(\mathbf{r}', t') \rangle = 0, \tag{4}$$

where indicies n,m,l runs over all tensor components. The average is performed over independent initial conditions, and the properties in Equation (4) follow the principles of stochastic forcing [17]. Substituting Equation (3) into Equation (2) we arrive at the dynamical equation for the polarisation density

$$\frac{\partial \rho\mathbf{p}}{\partial t} + \nabla \cdot \big(\rho\mathbf{u}\mathbf{p}\big) = \frac{1}{\tau_P}\big(\kappa\mathbf{E} - \rho\mathbf{p}\big) + \rho(\boldsymbol{\Omega} \times \mathbf{p}) + \chi_l \nabla(\nabla \cdot \mathbf{p}) + \chi_t \nabla^2 \mathbf{p} - \nabla \cdot \delta\mathbf{R}. \tag{5}$$

For convenience the coefficients $\chi_t = \chi_0 + \chi_r$ and $\chi_l = \chi_v + \chi_0/3 - \chi_r$ have been introduced.

We write the quantities in terms of the average and fluctuating parts, that is on the general form $A = \langle A \rangle + \delta A = A_{\text{av}} + \delta A$. To first order in the fluctuations Equation (5) then reduces to

$$\rho_{\text{av}} \frac{\partial \delta\mathbf{p}}{\partial t} = \frac{1}{\tau_P}\big(\kappa\delta\mathbf{E} - \rho_{\text{av}}\delta\mathbf{p}\big) + \chi_l \nabla(\nabla \cdot \delta\mathbf{p}) + \chi_t \nabla^2 \delta\mathbf{p} - \nabla \cdot \delta\mathbf{R}. \tag{6}$$

In Fourier space for wavevector $\mathbf{k}$, this is

$$\rho_{\text{av}} \frac{\partial \widetilde{\delta}\mathbf{p}}{\partial t} = \frac{1}{\tau_P}\Big(\kappa\widetilde{\delta}\mathbf{E} - \rho_{\text{av}}\widetilde{\delta}\mathbf{p}\Big) - \chi_l \mathbf{k}(\mathbf{k} \cdot \widetilde{\delta}\mathbf{p}) - \chi_t \mathbf{k}^2 \widetilde{\delta}\mathbf{p} - i\mathbf{k} \cdot \widetilde{\delta}\mathbf{R}. \tag{7}$$

We now choose the wavevector $\mathbf{k} = (k, 0, 0)$, and write the dynamics of each

vector component for the dipole moment explicitly as

$$\frac{\partial \widetilde{\delta p}_x}{\partial t} = \frac{1}{\tau_P}\left(\frac{\kappa}{\rho_{\text{av}}}\widetilde{\delta E}_x - \widetilde{\delta p}_x\right) - (\nu_l + \nu_t)k^2\widetilde{\delta p}_x - \frac{ik}{\rho_{\text{av}}}\widetilde{\delta R}_{xx} \tag{8a}$$

$$\frac{\partial \widetilde{\delta p}_y}{\partial t} = \frac{1}{\tau_P}\left(\frac{\kappa}{\rho_{\text{av}}}\widetilde{\delta E}_y - \widetilde{\delta p}_y\right) - \nu_t k^2\widetilde{\delta p}_y - \frac{ik}{\rho_{\text{av}}}\widetilde{\delta R}_{xy} \tag{8b}$$

$$\frac{\partial \widetilde{\delta p}_z}{\partial t} = \frac{1}{\tau_P}\left(\frac{\kappa}{\rho_{\text{av}}}\widetilde{\delta E}_z - \widetilde{\delta p}_z\right) - \nu_t k^2\widetilde{\delta p}_z - \frac{ik}{\rho_{\text{av}}}\widetilde{\delta R}_{xz}, \tag{8c}$$

where we have introduced the kinematic transport coefficients $\nu_t = \chi_t/\rho_{\text{av}}$ and $\nu_l = \chi_l/\rho_{\text{av}}$. With this choice of wavevector the dynamics separates into a longitudinal mode, Equation (8a), and a transverse mode, Equation (8b), or equivalently Equation (8c).

Multiplying Equation (8a) by $\delta p_x(-k, 0)$ and ensemble averaging over independent initial conditions we get

$$\frac{\partial C^{\parallel}_{pp}}{\partial t} = \frac{1}{\tau_P}\left(\kappa C^{\parallel}_{Ep} - C^{\parallel}_{pp}\right) - (\nu_t + \nu_l)k^2 C^{\parallel}_{pp}, \tag{9}$$

where $C^{\parallel}_{pp}$ is the normalised longitudinal dipole autocorrelation function

$$C^{\parallel}_{pp}(k, t) = \frac{\langle \delta p_x(k, t)\delta p_x(-k, 0)\rangle}{\langle \delta p_x(k, 0)\delta p_x(-k, 0)\rangle}, \tag{10}$$

and $C^{\parallel}_{Ep}$ the normalised longitudinal electric field dipole correlation function

$$C^{\parallel}_{Ep}(k, t) = \frac{\langle \delta E_x(k, t)\delta p_x(-k, 0)\rangle}{\langle \delta E_x(k, 0)\delta p_x(-k, 0)\rangle}. \tag{11}$$

Likewise, multiplying Equation (8b) by $\delta p_y(-k, 0)$ and ensemble averaging we get an equation for the corresponding transverse correlation functions

$$\frac{\partial C^{\perp}_{pp}}{\partial t} = \frac{1}{\tau_P}\left(\frac{\kappa}{\rho_{\text{av}}}C^{\perp}_{Ep} - C^{\perp}_{pp}\right) - \nu_t k^2 C^{\perp}_{pp}. \tag{12}$$

with

$$C^{\perp}_{pp}(k, t) = \frac{\langle p_y(k, t)p_y(-k, 0)\rangle}{\langle p_y(k, 0)p_y(-k, 0)\rangle} \quad \text{and} \quad C^{\perp}_{Ep}(k, t) = \frac{\langle E_y(k, t)p_y(-k, 0)\rangle}{\langle E_y(k, 0)p_y(-k, 0)\rangle}. \tag{13}$$

The two differential equations, Equations (9) and (12), are of the same form and therefore have the same general solution. If we let α refer to either the

longitudinal or the transverse correlation functions, we can write the solution as

$$C^{\alpha}_{pp}(k,\,t) = \mathrm{e}^{-(1/\tau_P+\nu_\alpha k^2)t}\left[C_0 + \frac{\kappa}{\tau_P \rho_{\mathrm{av}}}\int C^{\alpha}_{Ep}(k,\,t)\,\mathrm{e}^{(1/\tau_P+\nu_\alpha k^2)t}\,\mathrm{d}t\right] \tag{14}$$

in which $\nu_\alpha = \nu_t + \nu_l$ in the longitudinal case and $\nu_\alpha = \nu_t$ in the transverse case. C_0 is a constant of integration and found from the initial condition $C^{\alpha}_{pp}(k,\,0) = 1$.

The solution has one unknown function, namely, $C^{\alpha}_{Ep}(k,\,t)$. If $\mathbf{E}$ is the macroscopic local electric field, a natural approach is to invoke the Maxwell equations. Especially, in the case of a zero free-charge density Gauss' law states a zero divergence of the electrical displacement field, $\nabla \cdot \mathbf{D} = 0$, that is, the local electric field is given through the local polarisation and C^{α}_{Ep} is directly related to C^{α}_{pp}. This relation will not be true in the general case and we let $\mathbf{E}$ be a generalised microscopic local field by letting

$$C^{\alpha}_{Ep}(k,\,t) = A_\alpha(k)\,\mathrm{e}^{-t/\tau_E} \tag{15}$$

in which A_α is wavevector dependent amplitude. In general, we write this on the form $A_\alpha = A_0 + A_{1,\alpha}k + A_{2,\alpha}k^2 + \ldots$ such that the coupling between the field and polarisation is the same for the longitudinal and transverse dynamics in the limit of zero wavevector. τ_E is the characteristic correlation time which we assume is the same for the longitudinal and transverse dynamics for all wavevectors. Substituting the ansatz, Equation (15), for C_{Ep} into Equation (14) yields

$$C^{\alpha}_{pp}(k,\,t) = C_0\,\mathrm{e}^{-(1/\tau_P+\nu_\alpha k^2)\,t} + \frac{\kappa A_\alpha(k)\,\mathrm{e}^{-t/\tau_E}}{\rho_{\mathrm{av}}(1+\nu_\alpha k^2\tau_P - \tau_P/\tau_E)}. \tag{16}$$

Since $C^{\alpha}_{pp}(k,\,0) = 1$, the constant of integration is readily found and one ends up with the particular solution

$$C^{\alpha}_{pp}(k,\,t) = \frac{\kappa A_\alpha(k)}{\rho_{\mathrm{av}} b}\,\mathrm{e}^{-t/\tau_E} - \left[\frac{\kappa A_\alpha(k)}{\rho_{\mathrm{av}} b} - 1\right]\mathrm{e}^{-(1/\tau_P+\nu_\alpha k^2)\,t}, \tag{17}$$

where $b = 1 + \nu_\alpha k^2\tau_P - \tau_P/\tau_E$.

In order to compare the model to numerical data for the dielectric permittivity we note that the Fourier-Laplace transformation of Equation (17) is given by

$$\begin{aligned}\widehat{C}^{\alpha}_{pp}(k,\,\omega) &= \int_0^\infty C^{\alpha}_{pp}(k,\,t)\mathrm{e}^{-i\omega t}\mathrm{d}t \\ &= \frac{\kappa A_\alpha(k)}{\rho_{\mathrm{av}} b}\frac{1}{1/\tau_E + i\omega} - \left[\frac{\kappa A_\alpha(k)}{\rho_{\mathrm{av}} b} + 1\right]\frac{1}{1/\tau_P + \nu_\alpha k^2 + i\omega}\end{aligned} \tag{18}$$

and generalising the frequency-dependent permittivity [18, 19]

$$\varepsilon^{\alpha}_r(k,\,\omega) = \Delta\varepsilon_r\left[1 - i\omega\widehat{C}^{\alpha}_{pp}(k,\,\omega)\right], \tag{19}$$

where $\Delta\varepsilon$ is the so-called relaxation strength [19]. For the longitudinal permittivity the straightforward generalisation in Equation (19) is an approximation at low wavevectors to the true statistical mechanical formulation and will not feature the singularities shown by Bopp et al. [15].

Before comparing the model to molecular simulations data a few points are worth highlighting. (i) The model predicts two peaks in the dielectric loss (as defined by Equation (19), one Debye-type peak with frequency $1/\tau_P + \nu_\alpha k^2$ and the other with peak frequency $1/\tau_E$. We denote these the primary and secondary peaks, respectively. We adopt this terminology as the peaks may not be identical to the α and β peaks reported elsewhere in the literature, see also discussion below. (ii) In the low wavevector regime, the primary peak frequency increases as the wavevector squared. The secondary peak is wavevector independent. (iii) The primary peak is due to two processes, namely, a wavevector-independent Debye relaxation process and a diffusion process which tends to remove any dipole gradients in the system. (iv) The secondary peak is due to the coupling between the local microscopic field and the dipole moment.

3. Molecular dynamics and comparison

The molecular model is an ensemble of simple dumbbells, where one bead is positively charged and the other negatively charged. The charge magnitude is set to q=1e, where e is the unit of charge. The two beads are connected with a stiff spring such that the distance between them is on average $l = 1\sigma$, where σ is the characteristic length. The spring constant is k=1000 $(m\sigma)^2/\varepsilon$, where m is the mass of a bead and ε is the energy scale. With this stiffness we can safely ignore molecular elongation and assume that the molecular dipole moment magnitude is constant. Beads not belonging to the same molecule interact through the standard 6–12 Lennard–Jones and Coulomb potentials [20, 21]. To reduce the computational time the Coulomb interactions are approximated by the shifted force scheme [22–24], with a cut-off of $r_c = 6\sigma$. The bead number density is kept fixed at $n = 0.85\sigma^{-3}$, and we vary the temperature in the range $0.125\epsilon/k_B \leq T \leq 1.0\epsilon/k_B$. At lower temperatures the system crystallises within the simulation time frame used. The particles' equation of motion are integrated forward in time using the leap-frog algorithm with a Nosé–Hoover thermostat [25]. The time step is $\Delta t = 0.002/(\sigma\sqrt{m/\epsilon})$ and we simulate the system for 10^8 time steps. In all simulations, 1000 molecules were studied; the system size dependence was checked against a system with 5000 molecules at temperature $T = 0.2\epsilon/k_B$ and zero wavevector, showing no size effects except from the phonon modes. From here on we omit writing the units explicitly.

It is informative to first look at the structure and dynamics of the molecular model. In Figure 1(a), the mean-square displacement is plotted for four different temperatures. This indicates that while the single molecule motion is indeed slowed down upon cooling (the diffusion is lowered by two orders of

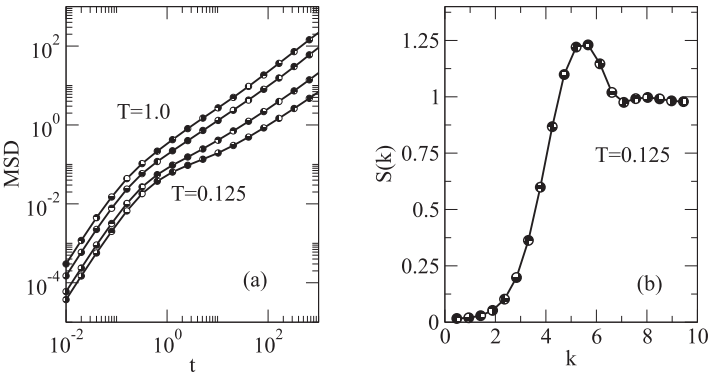

Figure 1. (a) Molecular mean-square displacement for four different temperatures, T=1.0,0.5,0.2 and 0.125. (b) Structure factor for T=0.125.

magnitude), the system is fluidic and does not enter an arrested state. The structure factor, Figure 1(b), is calculated from the coherent scattering function, $S(\mathbf{k}) = F(\mathbf{k}, 0)$, where

$$F(\mathbf{k}, t) = \frac{1}{N}\left\langle \widetilde{n}(\mathbf{k}, t)\widetilde{n}(-\mathbf{k}, 0)\right\rangle, \tag{20}$$

N being the total number of molecules in the system and $\widetilde{n}(\mathbf{k}, t) = \sum_i \mathrm{e}^{-\mathbf{k}\cdot\mathbf{r}_i}$ is the Fourier transformed number density; $\mathbf{r}_i$ is the centre-of-mass position of molecule i, and $\mathbf{k} = (k, 0, 0)$ as above. Clearly, the system only features short-ranged local structures.

The polarisation density is define microscopically as

$$\mathbf{P}(\mathbf{r}, t) = \rho(\mathbf{r}, t)\mathbf{p}(\mathbf{r}, t) = \sum_i \boldsymbol{\mu}_i \delta(\mathbf{r} - \mathbf{r}_i(t)), \tag{21}$$

where $\boldsymbol{\mu}$ is the molecular dipole moment (here with a magnitude of one), and δ is the Dirac delta not to be confused with the thermal fluctuation terms above. To first order in the fluctuations, we therefore have for the wavevector-dependent dipole moment

$$\widetilde{\delta}\mathbf{p}(\mathbf{k}, t) = \frac{1}{\rho_{\mathrm{av}}}\sum_i \boldsymbol{\mu}_i \,\mathrm{e}^{-i\mathbf{k}\cdot\mathbf{r}_i(t)}. \tag{22}$$

From Equations (10) and (13), we can the evaluate the dipole autocorrelation functions. As an example we plot in Figure 2 data for $C_{pp}^{\perp}$ and $C_{pp}^{\parallel}$ at T=0.2 and wavevectors $\mathbf{k} = \mathbf{0}$ and $\mathbf{k} = (1.42, 0, 0)$. Two important points should be noted. First, for zero wavevector the two correlation functions are the same within statistical uncertainty. This is in agreement with the model assumption that $A\alpha = A_0$ and by substituting $\mathbf{k} = \mathbf{0}$ in to Equation (17). Second, for non-zero wavevector the longitudinal dipole relaxation is faster than the transverse dipole relaxation. This is also in agreement with the model predictions as the

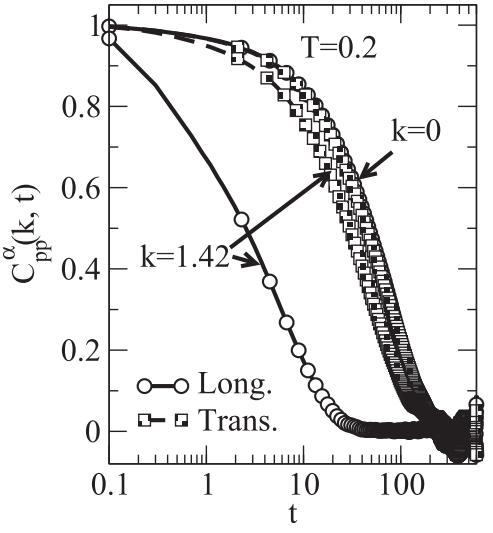

Figure 2. Dipole moment autocorrelation functions for wavevectors $\mathbf{k} = \mathbf{0}$ and $\mathbf{k} = (1.42, 0, 0)$. T=0.2. Lines connecting the data points (not all point shown) serve as a guide to the eye.

wavevector-dependent relaxation is determined by the kinematic transport coefficient. For the longitudinal relaxation, we have $\nu_{\parallel} = \nu_t + \nu_l$, which is always larger than or equal to the transverse case, $\nu_{\perp} = \nu_t$, that is, $\nu_{\perp} \leq \nu_{\parallel}$.

From the dipole relaxation functions, $C^{\perp}_{pp}$ and $C^{\parallel}_{pp}$, we can evaluate the corresponding dielectric permittivities defined here by Equation (19). Figure 3(a) shows the temperature dependence of the dielectric loss. For T=1.0 one observes one main peak; this peak shifts to lower frequencies as the temperature decreases. As this shift occurs, a second peak emerges and the peak position is less dependent of temperature. These two temperature characteristics are also observed for the α and β peaks, see Ref. [10] and references therein. The fact that the second peak's relative amplitude increases with decreasing temperature has been reported for the β-peak in a decahydroisoquinoline liquid [11]. From Figure 3(b), one also observes that the first peak's position is wavevector dependent, whereas the second peak is not. This is in agreement with the model predictions above and we therefore associate the peaks with the model's primary and secondary peaks.

According to the model, the primary peak frequency is due to a diffusive process, hence, the frequency should increase as the wavevector squared for low wavevectors. This is confirmed for T=1.0, Figure 3(c). At lower temperatures, the kinematic transport coefficients ν_t and ν_l become wavevector dependent [26], and the simple dispersion relation no longer holds.

At frequencies just below 20 one also observes a third weak peak, which is approximately independent of wavevector and weakly dependent of temperature. This mode is shown in more details in Figure 3(d). This mode is system size dependent (at least for zero wavevector) and is also present if the bond

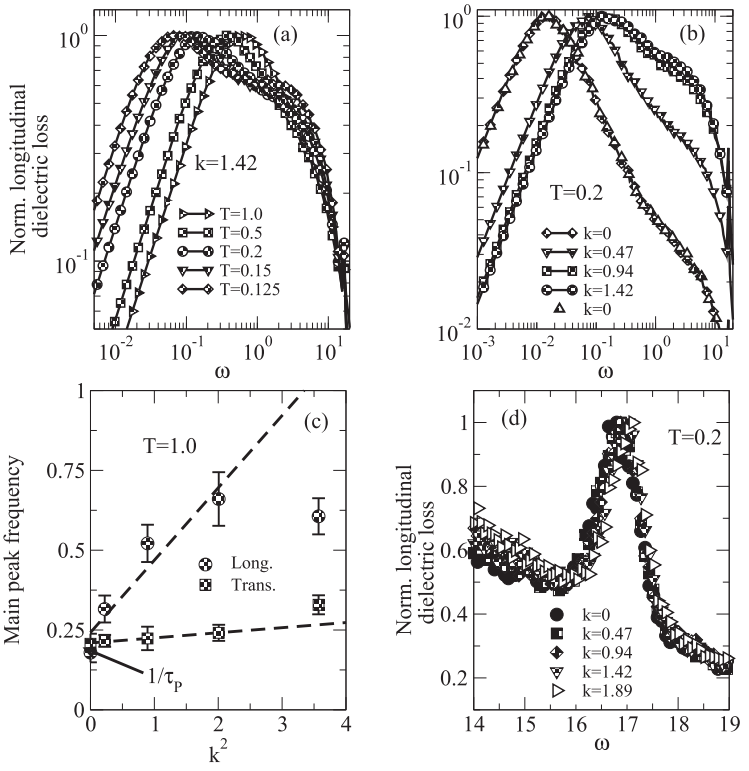

Figure 3. (a) The normalised dielectric loss as a function of frequency for different temperatures at $\mathbf{k} = (1.42, 0, 0)$. (b) The normalised dielectric loss as a function of frequency for different wavevectors at T=0.2. The dotted filled triangles represent data for the large system using 5×10^3 molecules; no size effect can be observed. The axis scales are changed in (a) and (b) in order to highlight the relevant details. Lines serve as a guide to the eye. (c) Dispersion relations for the primary at T=1.0. (d) Phonon mode at large frequencies. T=0.2.

connecting the beads is rigid, i.e. it cannot be due to an intra-molecular vibrational mode. We therefore assign this frequency to the characteristic system phonon frequency. Furthermore, we note that the acoustic phonon mode is wavevector dependent. We therefore argue that the secondary peak is not a phonon.

From data one can fix the relaxation times τ_P, and then use τ_E, ν_α and the amplitude κA as fitting parameters. In Figure 4, we show four examples of this fitting protocol; the model fits agree well with the molecular dynamics data.

As discussed above, if one fits the model to data at low temperature and different wavevectors, the kinematic transport coefficients are wavevector dependent; we leave this investigation to further work. However, the two characteristic times for the primary and secondary peaks can be extracted directly from data and we show the result in Figure 5. Clearly, the temperature dependencies of τ_P and τ_E are different; as mentioned above, the fact that the secondary peak's temperature dependence is lower than the primary peak's is in agreement with

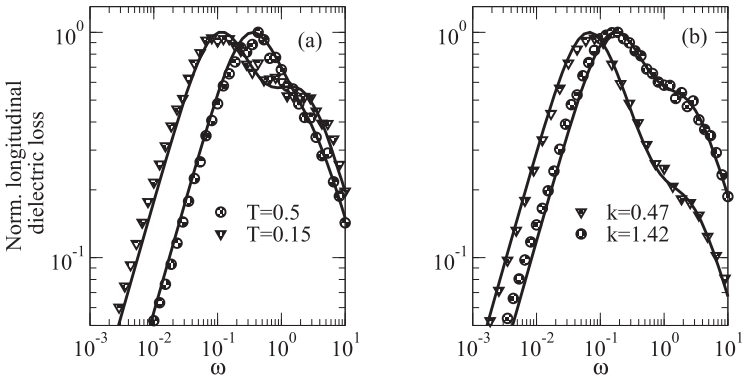

Figure 4. Comparison between the molecular dynamics results (symbols) and the model (full lines) using τ_E, $\nu_\alpha = \nu_t + \nu_l$ and κA as fitting parameters.

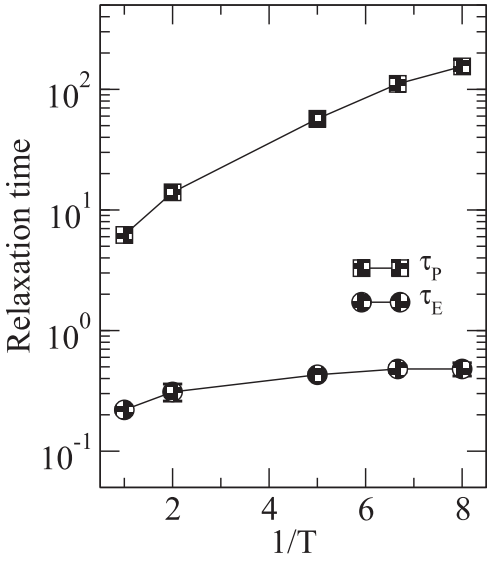

Figure 5. The two characteristic relaxation times for different temperatures. Lines serve as a guide to the eye.

the typical α and β behaviour in super-cooled liquids [9, 12]. However, for the present dielectrics this dependency is concave, and not convex as often observed in experiments.

4. Conclusion

We have performed molecular dynamics simulations of a molecular model for a simple dielectric fluidic material. From the simulations, we extract the longitudinal and transverse dielectric loss as defined here from the approximation in Equation (19) as functions of both frequency and wavevector. The dielectric

loss features three peaks, a primary, a secondary and a phonon peak. The purpose of the paper was then to compare the simulation data to a mechanistic model based on the balance equation for the polarisation density.

In agreement with the simulation data, the model predicts (i) that the transverse and longitudinal permittivities are the same functions of frequency at zero wavevector, (ii) that for non-zero wavevector the polarisation relaxation is fastest for the longitudinal mode, (iii) that there exists two non-phonon modes (two peaks in the dielectric loss), and that (iv) for low wavevector and sufficiently large temperatures the dispersion relation for the primary peak goes as the wavevector squared.

It is not clear whether the primary and secondary peaks correspond to the α and β peaks reported in the literature for super-cooled liquids. First, these peaks are usually associated with glassy systems, that is, where the molecular dynamics is extremely slow. In the present model system this is not the case, Figure 1. Secondly, usually the β peak amplitude decreases with increasing temperature, where we observe the opposite behaviour for the present model. Finally, the characteristic relaxation times τ_P and τ_E show a concave dependency with respect to the inverse of temperature; this also does not agree with what is most often found experimentally.

Acknowledgments

This work was supported by the VILLUM Foundation's grant Matter (16515).

Disclosure statement

No potential conflict of interest was reported by the author(s).

Funding

This work was supported by the VILLUM Foundation's (Villum Fonden) grant Matter (16515).

References

[1] S.R. de Groot and P. Mazur, *Non-Equilibrium Thermodynamics*, Dover Publications, New York, 1984.
[2] J.P. Hansen and I.R. McDonald, *Theory of Simple Liquids*, Academic Press, Amsterdam, 2006.
[3] V. Ballenegger and J.P. Hansen, *Dielectric permittivity profiles of confined polar fluids*, J. Chem. Phys. 122 (2005), p. 114711.
[4] P.J.W. Debye, *Polar Molecules*, The Chemical Catalog Company, Inc., New York, 1929.
[5] G.P. Johari and M. Goldstein, *Viscous liquids and the glass transition. II. Secondary relaxations in glasses of rigid molecules*, J. Chem. Phys. 53 (1970), p. 2372.

[6] G.P. Johari and M. Goldstein, *Viscous liquids and the glass transition. III. Secondary relaxations in aliphatic alcohols and other nonrigid molecules*, J. Chem. Phys. 55 (1971), p. 4245.
[7] F. Kremer and A. Schönhals (eds.), *Broadband Dielectric Spectroscopy*, Springer, Berlin, 2003.
[8] J.C. Dyre and N.B. Olsen, *Minimal model for beta relaxation in viscous liquids*, Phys. Rev. Lett. 91 (2003), p. 155703.
[9] C.M. Roland and R. Casalini, *Dynamics of Poly(cyclohexyl methacrylate): Neat and in blends with Poly(alpha-methylstyrene)*, Macromolecules 40 (2007), p. 3631.
[10] C.M. Roland, *Viscoelastic Behavior of Rubbery Materials*, Oxford University Press, Oxford, 2011.
[11] B. Jakobsen, K. Niss, and N.B. Olsen, *Dielectric and shear mechanical alpha and beta relaxations in seven glass-forming liquids*, J. Chem. Phys. 123 (2005), p. 234511.
[12] G. Floudas, M. Paluch, A. Grzybowski, and K.L. Ngai, *Molecular Dynamics of Glass-Forming Systems*, Springer, Heidelberg, 2011.
[13] J.S. Hansen, A. Kisliuk, A.P. Sokolov, and C. Gainaru, *Identification of structural relaxation in the dielectric response of water*, Phys. Rev. Lett. 116 (2016), p. 237601.
[14] J.G. Kirkwood, *The dielectric polarization of polar liquids*, J. Chem. Phys. 7 (1939), pp. 911–919.
[15] P.A. Bopp, A.A. Kornyshev, and G. Sutmann, *Frequency and wave-vector dependent dielectric function of water: Collective modes and relaxation spectra*, J. Chem. Phys. 109 (1998), p. 1939.
[16] J.S Hansen, *Reduced dielectric response in spatially varying electric fields*, J. Chem. Phys. 143 (2015), p. 194507.
[17] J.M.O. de Zárate and J.V. Sengers, *Hydrodynamic Fluctuations*, Elsevier, Amsterdam, 2006.
[18] D.M.F. Edwards, P.A. Madden, and I.R. McDonald, *A computer simulation study of the dielectric properties of a model of methyl cyanide*, Mol. Phys. 51 (1984), p. 1141.
[19] G.D. Smith, O. Borodin, and W. Paul, *A molecular-dynamics simulation study of dielectric relaxation in a 1,4.polybutadiene melt*, J. Chem. Phys. 117 (2002), p. 10350.
[20] D.A. McQuarrie, *Statistical Mechanics*, Harper and Row, New York, 1976.
[21] M.P. Allen and D.J. Tildesley, *Computer Simulation of Liquids*, Clarendon Press, New York, 1989.
[22] D. Wolf, P. Keblinski, S.R. Phillpot, and J. Eggebrecht, *Exact method for the simulation of Coulombic systems by spherically truncated, pairwise r^{-1} summation*, J. Chem. Phys. 110 (1999), p. 8254.
[23] C.J. Fennell and J.D. Gezelter, *Is the Ewald summation still necessary? Pairwise alternatives to the accecpted standard for long-ranged electrostatics*, J. Chem. Phys. 124 (2006), p. 234104.
[24] J.S. Hansen, T.B. Schrøder, and J.C. Dyre, *Simplistic Coulomb forces in Molecular Dynamics: Comparing the Wolf and Shifted-Force Approximations*, J. Phys. Chem. B 116 (2012), p. 5738.
[25] N.P. Bailey, T.S. Ingebrigtsen, J.S. Hansen, A.A. Veldhorst, L. Bøhling, C.A. Lemarchand, A.E. Olsen, A.K. Bacher, L. Costigliola, U.R. Pedersen, H. Larsen, J.C. Dyre, and T.B. Schrøder, *RUMD: A general purpose molecular dynamics package optimized to utilize GPU hardware down to a few thousand particle*, SciPost Phys. 3 (2017), p. 038.
[26] J.S. Hansen, *Multiscale dipole relaxation in dielectric materials*, Mol. Sim. 42 (2016), p. 1364.